

Supplementary Information for “Electron Transport from Quantum Kinetic Monte Carlo Simulations”

Fei Lin,^{*,†,‡} Jianqiu Huang,^{*,†} and Celine Hin^{*,†,¶}

[†]*Department of Mechanical Engineering, Virginia Tech, Blacksburg, Virginia 24061 USA*

[‡]*Department of Physics, Virginia Tech, Blacksburg, Virginia, 24061 USA*

[¶]*Department of Materials Science and Engineering, Virginia Tech, Blacksburg, Virginia 24061 USA*

E-mail: feilin@vt.edu; jianqiu@vt.edu; celhin@vt.edu

Absence of Sign Problem in 1D Hubbard Model

In this section we show that there is no sign problem in QKMC simulation with a 1D Fermi Hubbard model. We define a propagated state $|\alpha(p)\rangle = |\alpha_{\uparrow}(p)\alpha_{\downarrow}(p)\rangle$ along the imaginary-time evolution of state in SSE.¹ Index p means p operators have been applied on an initial electron configuration $|\alpha(0)\rangle$, i.e.,

$$|\alpha(p)\rangle \sim \prod_{i=1}^p H_{b_i} |\alpha(0)\rangle \quad (\text{S1})$$

We also order the electrons in the state representation so that up-spin creation operators precede the down-spin creation operators. When a diagonal operator, e.g., $n_{i,\sigma} = c_{i,\sigma}^{\dagger} c_{i,\sigma}$ acts on the propagated state, there is a phase factor $(-1)^{2N_{\uparrow}^i}$ if $\sigma = \uparrow$ or $(-1)^{2N_{\uparrow}^i + 2N_{\downarrow}^i}$ if $\sigma = \downarrow$, where $N_{\uparrow,\downarrow}^i$ is the number of up- or down-spin electrons appearing on lattice site with site

index $j < i$, and N_{\uparrow} is total number of up-spin electrons in the system. In either case, the factor -1 introduced by Fermi statistics always appear twice in the phase factor, leading to a $+1$ phase factor. When an off-diagonal operator acts on the state, the same phase factors are introduced if open boundary condition (OBC) is used. Consequently, there is no sign problem in QKMC simulation for the 1D Fermi Hubbard model with OBC.

QKMC for Canonical System

QMC simulation with SSE method is usually carried out in grand canonical systems, where total number of particles can fluctuate. However, if we want to calculate electric current going from the left to the right across the interface in our system (see Fig. 1 in the main text), we should perform QKMC in a canonical system, i.e., by setting $N_L + N_R$ to a fixed value. At half-filling for a 20-site system, for example, $N_L + N_R = 20$.

Diagonal update discussed in the main text keeps the total number of electrons fixed; while off-diagonal update may change the electron number. Off-diagonal transitions that change the total number of electrons in the system will then be rejected.

Solution to Detailed Balance Equation

As mentioned in the main text, there are infinite number of solutions² to the detailed balance equation such as:

$$\frac{W_i}{W_{i-1}} = \frac{p(W_{i-1} \rightarrow W_i)}{p(W_i \rightarrow W_{i-1})}, \quad (\text{S2})$$

where W_{i-1} (W_i) is the old(new) configuration for a specific bond operator in the directed loop.

Here we explore two specific solutions: heat-bath (HB) and bounce-free (BF) or bounce-minimization solutions.¹ Suppose that for a specific bond with an old configuration weight W_1 , i.e., W_{i-1} , it can exist up to 3 new possible configurations W_2 , W_3 , and W_4 , which are

generated from the old configuration according to particle number conservation. Anyone of the 3 configurations could be the new configuration W_i . All 4 configuration weights are related by the following directed loop equation:

$$\begin{pmatrix} a_{11} & a_{12} & a_{13} & a_{14} \\ a_{12} & a_{22} & a_{23} & a_{24} \\ a_{13} & a_{23} & a_{33} & a_{34} \\ a_{14} & a_{24} & a_{34} & a_{44} \end{pmatrix} \begin{pmatrix} 1 \\ 1 \\ 1 \\ 1 \end{pmatrix} = \begin{pmatrix} W_1 \\ W_2 \\ W_3 \\ W_4 \end{pmatrix}, \quad (\text{S3})$$

where a_{ij} forms a real symmetric matrix as ensured by the detailed balance equation and is given by:

$$a_{ij} = W_i p(W_i \rightarrow W_j). \quad (\text{S4})$$

The HB solution to the directed loop equation gives:

$$a_{ij} = \frac{W_i W_j}{W_1 + W_2 + W_3 + W_4}. \quad (\text{S5})$$

To obtain BF or bounce-minimization solutions, we first rank W_i 's from the biggest to the smallest values: $W_1 > W_2 > W_3 > W_4$. The BF solution¹ is given by:

$$\begin{aligned} a_{12} &= (W_1 + W_2 - W_3 - W_4)/2, \\ a_{13} &= (W_1 - W_2 + W_3 - W_4)/2, \\ a_{14} &= W_4, \\ a_{23} &= (-W_1 + W_2 + W_3 + W_4)/2, \\ a_{24} &= 0, \\ a_{34} &= 0, \\ a_{ii} &= 0, \text{ for } i = 1, \dots, 4, \end{aligned} \quad (\text{S6})$$

if $W_1 < W_2 + W_3 + W_4$, or the bounce-minimization solution¹ is given by:

$$\begin{aligned}
a_{11} &= W_1 - W_2 - W_3 - W_4, \\
a_{1i} &= W_i, \text{ for } i = 2, \dots, 4, \\
a_{ij} &= 0, \text{ for others,}
\end{aligned} \tag{S7}$$

if $W_1 > W_2 + W_3 + W_4$.

QKMC for 2-Site System

To check our new QKMC algorithm, we perform grand canonical QKMC simulations in the equilibrium limit for a 2-site system. We first exactly diagonalize (ED) the 2-site system and compare the exact results with QKMC simulations with HB or BF updates. QKMC simulations were warmed up with 10^5 steps and data were collected over 16×10^5 QKMC steps. See Fig. S1 for comparisons. From the figure we see that ED results are in excellent agreement with the QKMC results, where two updating schemes (HB and BF) have been tested. In measuring the average energy and particle density in QKMC simulations, we have taken into account the time the system spends in one specific configuration, i.e., weighted by the cumulative time τ discussed in the main text. Since different updating schemes, HB and BF, have given consistent results, this means that the cumulative time τ is indeed real time that the system spends in a specific configuration. This is in contrast to the conventional QMC simulations with SSE, where the corresponding simulation time between two configurations or updating steps does not have the meaning of real time.

Electronic Band Structure of α Quartz

In this section we describe in detail our calculation of α quartz band structure using Vienna Ab initio Simulation Package (VASP) software package.^{3,4} First principle calculations have

been performed within the framework of Density Functional Theory (DFT) to study the band structure of α quartz. The Projector Augmented Wave (PAW) method has been used,^{5,6} as implemented in VASP. The plane wave cutoff energy for our calculations is set to 400 eV, and the self-consistent electronic loop is converged to 10^{-5} eV. The Local Density Approximation (LDA) exchange and correlation functional⁷ have been used to minimize the total energy. The conjugate gradient algorithm has been used to relax the atomic positions until forces on atoms are smaller than 1 meV/Å. In order to investigate the electronic structure quantitatively, PBE0 exchange and correlation functional⁸ have been used in the ultimate static calculation to correct the eigenlevel structure and the band gap in α quartz.

Figure S2 shows the band structure from our calculation. The indirect gap between valence and conduction bands is around 9 eV in good agreement with other calculated⁹ and experimental data.¹⁰

Hopping Integrals from MLWF

Since the electronic band structure was calculated in the previous section, we can proceed to determine the MLWFs for the α quartz system. We first run VASP to generate input files for Wannier90.¹¹ The number of Bloch bands N_B to be included in the Wannierization process^{12,13} depends on the applied electric potential difference V . The applied electric field induces holes in the valence bands. An equivalent picture to electron hopping with negative hopping integral is hole hopping with positive hopping integral. This is due to the electron-hole transformation $c_{i\sigma}^\dagger \rightarrow h_{i\sigma}$ and $c_{i,\sigma} \rightarrow h_{i,\sigma}^\dagger$, where $h_{i,\sigma}^\dagger$ ($h_{i\sigma}$) is the hole creation (annihilation) operator. Therefore, the kinetic energy part of the Hamiltonian becomes $-tc_{i,\sigma}^\dagger c_{i+1,\sigma} = -th_{i,\sigma} h_{i+1,\sigma}^\dagger = th_{i+1,\sigma}^\dagger h_{i\sigma}$. We should, therefore, look for positive hopping integrals among MLWFs.

Table S1 lists N_B together with V and the leading positive hopping integral t among MLWFs. Note that in obtaining hopping integrals we assume rigid band approximation

Table S1: Number of Bloch bands N_B involved in the Wannierization process and leading hopping integral t among MLWFs as a function of applied electric potential difference V .

V (eV)	N_B	t (eV)
0.8	2	0.048
2.36	5	0.116
2.66	8	0.331

because the applied electric field does not change the band structure of α quartz.

References

- (1) O. F. Syljuasen and A. W. Sandvik, Phys. Rev. E **66**, 046701 (2002).
- (2) F. Alet, S. Wessel and M. Troyer, Phys. Rev. E **71**, 036706 (2005).
- (3) G. Kresse and J. Furthmuller, Comput. Mat. Sci. **6**, 15 (1996).
- (4) G. Kresse and J. Furthmuller, Phys. Rev. B **54**, 11169 (1996).
- (5) P. E. Blochl, Phys. Rev. B **50**, 17953 (1994).
- (6) G. Kresse and D. Joubert, Phys. Rev. B **59**, 1758 (1999).
- (7) J. P. Perdew and A. Zunger, Phys. Rev. B **23**, 5048 (1991).
- (8) J. P. Perdew, M. Ernzerhof, and K. Burke, J. Chem. Phys. **105**, 9982 (1996).
- (9) J. R. Chelikowsky and M. Schluter, Phys. Rev. B **15**, 4020 (1977).
- (10) Z. A. Weinberg, G. W. Rubloff, and E. Bassous, Phys. Rev. B **19**, 3107 (1979).
- (11) A. A. Mostofi, J. R. Yates, G. Pizzi, Y. S. Lee, I. Souza, D. Vanderbilt and N. Marzari, Comput. Phys. Commun. **185**, 2309 (2014).
- (12) N. Marzari and D. Vanderbilt, Phys. Rev. B **56**, 12847 (1997).
- (13) I. Souza, M. Marzari, and D. Vanderbilt, Phys. Rev. B **65**, 035109 (2001).

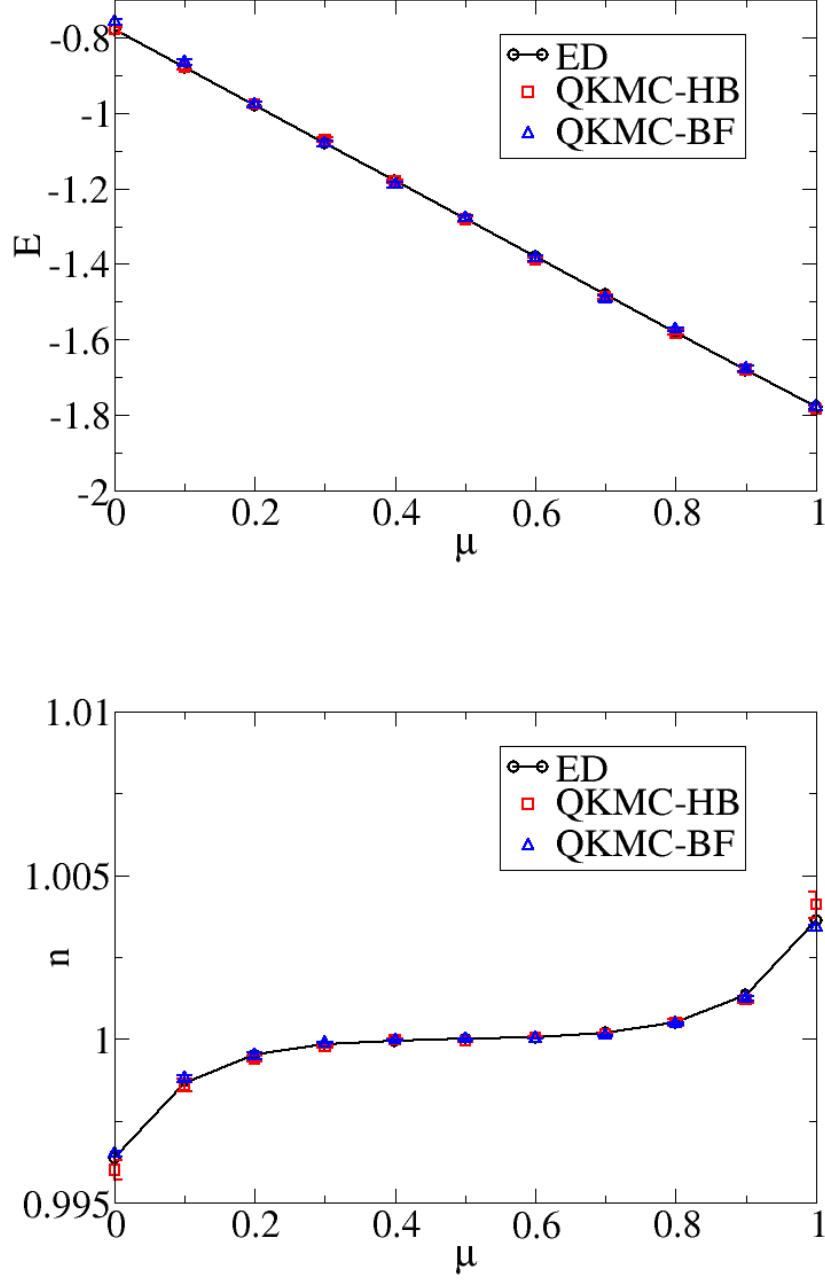


Figure S1: Comparison of energy (top panel) and particle number (bottom panel) per site between ED calculation and QKMC simulations with HB or BF updating schemes for a 2-site system with OBC. We have set $T/U = 0.1$, $t/U = 1.0$, and scanned a series of chemical potential values $\mu/U = 0.0, 0.1, \dots, 1.0$.

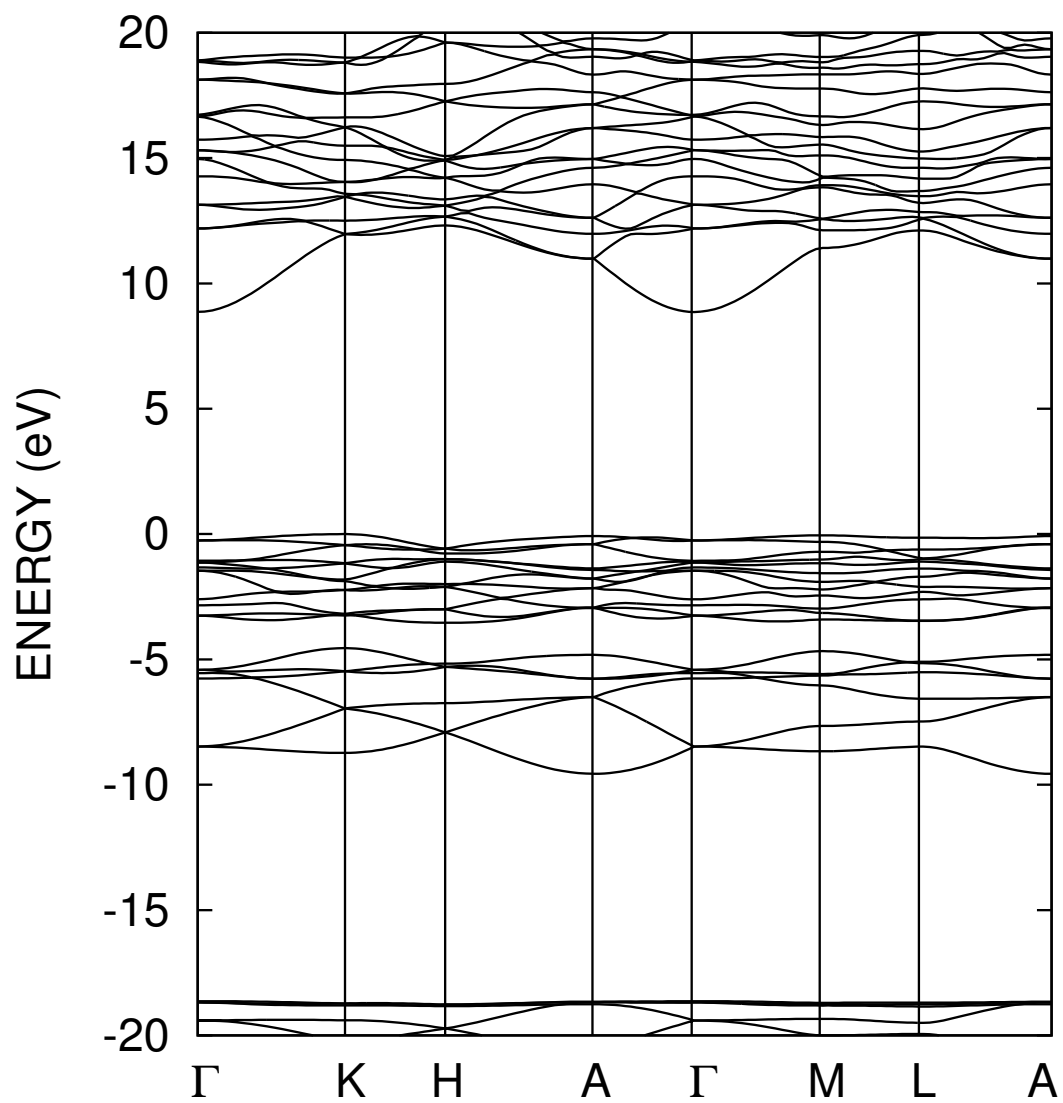


Figure S2: Electronic band structure for α quartz. Fermi energy is located at 0 eV.